In-Situ Monitoring of Additive Manufacturing

In-situ Monitoring of Additive Manufacturing

Davide Cannizzaro, Antonio Giuseppe Varrella, Stefano Paradiso,
Roberta Sampieri, Enrico Macii, Massimo Poncino, Edoardo Patti and
Santa Di Cataldo

Abstract Additive Manufacturing, in great part due to its huge advantages in terms of design flexibility and parts customization, can be of major importance in maintenance engineering and it is considered one of the key enablers of Industry 4.0. Nonetheless, major improvements are needed towards having additive manufacturing solutions achieve the quality and repeatability standards required by mass production. In-situ monitoring systems can be extremely beneficial in this regard, as they allow to detect faulty parts at a very early stage and reduce the need for post-process analysis. After providing an overview of Additive Manufacturing and of the state of the art and challenges of in-situ defects monitoring, this chapter describes an in-house developed system for detecting powder bed defects. For that purpose, a low-cost camera has been mounted off-axis on top of the machine under consideration. Moreover, a set of fully automated algorithms for computer vision and machine learning enables allow the timely detection of a number of powder bed defects along with the layer-by-layer monitoring of the part's profile.

1 Introduction

Additive manufacturing (AM) is the process of joining materials layer by layer to create objects, starting from a three-dimensional (3D) model. AM uses computer-aided-design (CAD) software to drive a 3D printer towards creating precise geometric shapes. Afterwards, the CAD model is converted into a series of layers and instructions suitable for a printer, and then the layers are printed sequentially. AM is one of the most promising manufacturing technologies [10] that are emerging in

Davide Cannizzaro, Antonio Giuseppe Varrella, Enrico Macii, Massimo Poncino, Edoardo Patti and Santa Di Cataldo
Politecnico di Torino, Italy, e-mail: name.surname@polito.it

Stefano Paradiso and Roberta Sampieri
FCA Product Development AM Centre, Turin, Italy. e-mail: name.surname@fcagroup.com

the context of Industry 4.0. The first machine for AM was developed in 1984 by Chuck Hull [25], the founder of 3D Systems, a well-known company that develops 3D printers. The first prototype was expensive thus making it inaccessible to the wide market. However, the constant improvements in hardware and software solutions, affecting their performance and reducing their cost, has results in the spread of 3D printers in many industrial fields [37]: in the past few years, many industries have already embraced AM technologies, and they are beginning to incorporate AM in their production lines and business models [31]. This is especially true for the medical, automotive and aerospace sectors, where AM is pushing forward innovative applications such as custom-made implants and prosthetic, as well as lightweight and complex components of cars and airplanes [12, 23, 33, 40]

The main advantages of AM over traditional technologies are mass customization, on-demand and decentralized manufacturing, freedom of design, and the ability to manufacture complex structures and fast prototyping. In other words, AM technology allows mass customization at low cost, implying that industries can design and personalize parts production with small efforts and without lengthy delivery time, or even have parts printed directly at the local distributors or service providers' premises, reducing the delivery time and the logistics requirements [36].

As it makes it possible to produce critical spare parts in small quantities at a very low cost and even to print such parts locally, AM technologies, together with predictive analytics and digitalization, could revolutionize the business models of maintenance industry and fulfill the potentials of condition-based maintenance (CbM) and predictive maintenance (PdM): in this scenario, heterogeneous sensors can be used to continuously monitor the condition of critical parts, and data-driven predictive models can be exploited to anticipate part failures and breakdowns, as well as to plan local repairs or replacements of the damaged parts by means of AM, with tremendous reduction of costs and time.

On the one hand, AM is considered one of the pillars of smart manufacturing and maintenance industry. On the other hand, it is still in the early stage of development [5]. Hence, it has some important drawbacks: build size limitations, long production time, high equipment and maintenance costs, along with a lack of quality assurance and process repeatability. Typically, an industrial 3D printer has a build volume ranging from $100mm^3$ to $400mm^3$, which only allows printing objects with a small size and packed effectively [11]. Due to this limitation, some parts require to be manufactured in segments and assembled at the end. Additionally, the average time to produce a single part is high [20], which currently makes AM more suitable to mass customization manufacturing than mass production. Moreover, 3D printer associated costs are higher when compared to traditional subtractive equipment. In this context, research efforts in the field of predictive maintenance of AM machines, which are currently at the very early stages, are expected to gain momentum in the future.

As mentioned before, one of the major barrier in the widespread of AM is the lack of quality assurance and repeatability. In particular, due to the complexity of additive processes and of the parts to be produced, some defects might occur during the printing process. To guarantee the quality standards required by industries (especially in

critical sectors like aerospace, automotive and healthcare) expensive and difficult post-process inspection are necessary. In order to address the aforementioned in an effective way, monitoring and control systems can be adopted for supervising the AM process during the layering procedure, enabled by sensors integrated with to the 3D printing machine. The real-time analysis of those sensor data can be useful for the early detection of defective parts, or even to correct the process in order to proactively address defects from occurring. In this regard, Machine Learning and Computer Vision (CV) analytics can significantly contribute.

Empowered by the aforementioned, the main focus of this chapter is in-situ defects monitoring in one of the most diffused metal AM technology, that is Direct Metal Laser Sintering (DMLS). In the following sections, a brief introduction of the main AM technologies available in the market is provided (Section 2), along with the state of the art in the field of monitoring systems (Section 3). Then, follows a near real-time AM monitoring system applied in an industrial use case, using visible-range cameras and computer vision algorithms (Section 4). Finally, the experimental results are discussed (Section 5) to conclude with Section 6.

2 Additive Manufacturing: process and methods

The main steps of a typical AM process are illustrated below in Fig. 1. It starts from a 3D CAD model of the products, then the model is converted into a stereolythography (STL) file format that describes the surface geometry of the object to be printed. The STL is processed by a slicer, a software that converts the model into a series of thin layers, and produces instructions tailored to a specific AM system. Finally, the final product may undergo a subtractive finishing process to achieve higher quality.

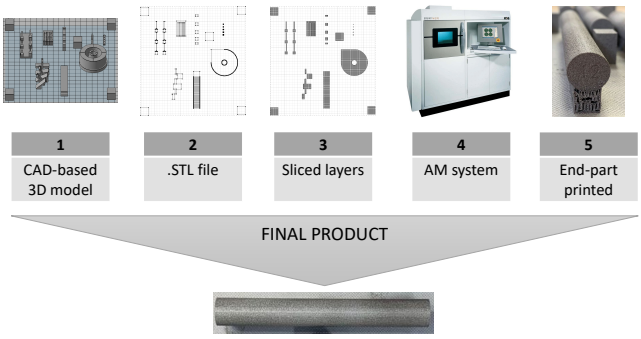

Fig. 1: AM Process: main phases.

In AM, many methods and materials are used to meet the demand for printing complex structures at fine resolutions. Fig. 2 shows the main technologies and the respective materials used. Stereolithography, Multi Jet Fusion, and Selective Laser Melting are intended for plastic materials. Instead, Fused Deposition Modelling and Laminated Object Manufacturing use both composite and plastic materials, while DMLS and Electron Beam Melting are suitable only for metal products.

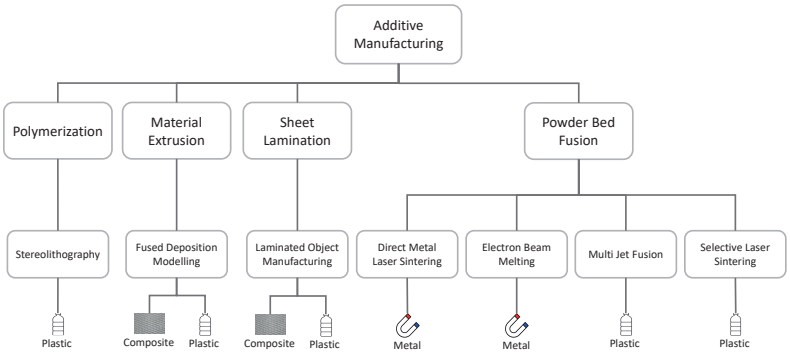

Fig. 2: AM technologies

The *Polymerization* process uses ultraviolet light to transform a plastic polymer from liquid to solid.

- *Stereolithography* is a liquid-based process that uses ultraviolet light (or electron beam) to initiate a chain reaction on a layer of photosensitive polymer [21]. Typically, a post-process treatment such as heating or photo-curing is required for some printed parts in order to achieve the desired mechanical performance. Stereolithography is suitable for high-quality parts with a fine resolution as low as $10\mu m$ [38]. However, it is relatively slow and expensive, suitable only for limited materials like resins that change their structure after intense exposure to ultraviolet light.

Material Extrusion is a process where a spool of material goes through a heated nozzle in a continuous stream to build a 3D object.

- *Fused Deposition Modeling* uses a continuous filament of a thermoplastic polymer to print an object. The process is based on the extrusion of a heated thermoplastic filament through a nozzle tip that deposits precisely the material on the platform to build the part. The main advantages are that no chemical post-processing or curing is required leading to an overall reduction of the costs [9]. However, the process does not allow high resolutions ($< 0.25mm$) with respect to other AM processes.

Sheet lamination is an AM methodology where thin sheets of material are bonded together to form a single piece that is cut into the desired 3D object.

- *Laminated Object Manufacturing* is one of the first commercial methods ever developed. It is based on a layer-by-layer cutting and lamination of sheets or rolls of material [28]. This process allows to reduce the cost of tooling and manufacturing time, and it is one of the most used AM methods for larger structures. However, Laminated Object Manufacturing has some disadvantages like inferior surface quality (without post-processing) and lower dimensional accuracy compared to the powder bed methods.

Powder Bed Fusion (PBF) involves spreading powder material on top of the previous layers through a recoater, with a reservoir providing new material supply. A heat source, typically a laser or electron beam, selectively melts together each layer of powder [16].

- *Direct Metal Laser Sintering* (DMLS) is one of the most used PBF technologies in AM, and hence is the main focus of this chapter. It allows to print parts with a 95% density without requiring any additional post-build sintering [22]. The DMLS process was developed by EOS GmbH, and it was first introduced in the EOS M250 machine in 1995. It uses a laser that is directly exposed to the metal powder in liquid phase sintering. Fig. 3 depicts the schematic picture of the instrument used for DMLS. The chamber is filled with an inert gas to avoid oxidation of the powder. The powder bed is heated to almost the melting point of the material and it is controlled by a piston that is lowered the same amount of the layer thickness each time a layer is finished. The powder allocated in the powder source chamber is spread using a recoater. The excess powder is removed and then the laser fused the powder at a specific location for each layer specified by the design. Nowadays, DMLS is the most widespread technique for metal, thanks to its trade-off between printing accuracy and cost [7].

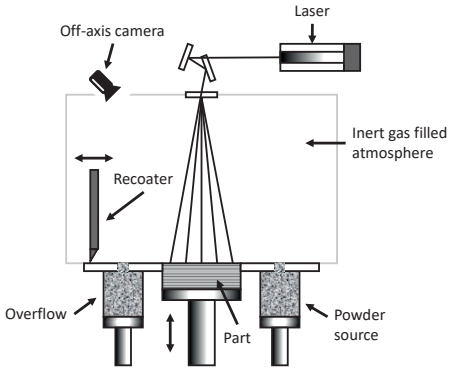

Fig. 3: DMLS set-up.

- *Electron Beam Melting* is a relatively novel process that involves an electron laser beam powered by high voltage in the range of $30 - 60kV$ to melt the powder [29]. The process is similar to DMLS but, in this process, the part is printed in a high vacuum chamber to avoid oxidation. Due to the high power produced by the laser, the penetration depth in the powder bed is greater with respect to DMLS. This high power could lead to the formation of cracks on the surface of the material, reducing the process stability.
- *Multi Jet Fusion* is an AM method developed by Hewlett-Packard. It creates parts additively thanks to a multi-agent printing process. Multi Jet Fusion manufacturing technique is particularly useful to create unique plastic parts with a good surface finish [17]. However, only a few plastic materials are suitable for the Multi Jet Fusion method.
- *Selective Laser Sintering* (SLS) is another printing process similar to DMLS, where a powder is sintered or fused by applying a laser beam. While DMLS is suitable only for metals, SLS can be used with various polymers. The main disadvantage compared to DMLS is that the accuracy is limited by the size of particles of the material. However, it allows a fine resolution and high quality for printing complex structures [1].

3 In-situ monitoring: current solutions

To this date, many AM systems do not have the capability to assess the quality of their products that they produce, unless with time-consuming and expensive post-process analysis. This majorly affects the overall time and cost of the production. To address this issue, many AM companies are providing software for near real-time visualization and monitoring of several process parameters. Nonetheless, these commercial solutions are generally limited in their scope: they do not develop a fully automated quality control strategy, and they fail to detect minor defects in the printed part [8]. Moreover, they are either not available on older machine models that are currently used by manufacturers, or typically require an expensive and complex set-up process.

Even though the data processing capabilities are still limited, most of the machines that are now available on the market allow to keep track of the history and behavior of the most important parameters of the machine for the entire job process. These parameters are related to either basic process conditions like laser power, build platform temperature, process chamber and ambient atmosphere, recoater speed, etc. or machine conditions like cooling system status, electrical power levels, powder source level, etc. [26]. Up-to-date machines can also be equipped with increasingly complex hardware like high-speed and infrared cameras, thermocouples, pyrometers, photo-detectors, that allow to monitor directly or indirectly many process parameters that are involved into the generation of defects.

Taking advantage of such advanced sensors, researchers are using an increasing amount of data analytics approaches to address the problem of AM monitoring and

control, mostly combining off-line Machine Learning (ML) methods with other types of algorithms, depending on the nature of the sensor data [6, 24, 42].

With the use of optical sensors (either in the visible or in the Infra-Red range) to acquire images of the build chamber, many approaches combine ML together with Computer Vision algorithms to perform AM defect analysis. For example, in [34] the authors propose a Convolutional Neural Network (CNN) for autonomous detection and classification of different type of anomalies. They extract the relevant features from the images and train the algorithm to detect possible part damages, incomplete spreading of powder, and recoating errors. In [3], the authors propose an online monitoring algorithm that uses computer vision to detect defect formation in every layer of the PBF process. They collect a set of images with a high-resolution camera, and analyze the images to detect layers with low quality of fusion or defects. In [41], the authors utilized a high-speed camera to acquire the powder bed images. Then, they combined a Support Vector Machines with a CNN to analyze the images and detect possible defects during the printing process.

Other researches focus on more unconventional types of data sources. For example, in [35, 39] PBF defects are detected based on acoustic emissions acquired by either microphones of optical fibers, using different types of neural networks like Deep Belief Networks or Spectral Convolutional Neural Networks for the classification task. Finally, in [15], heterogeneous data from a combination of different sensors are collected from the laser system, powder bed and recoating process in an Electron Beam Melting system, and then fed into a Support vector data description (SVDD) model to find major deviations from the expected pattern (e.g., cracks and holes on the surface). A disadvantage of the latter approaches is that they generally require invasive modification on the machine and expensive hardware additions for the data collection.

Recent literature demonstrates data-driven techniques being promising to monitor and improve AM processes. Nonetheless, the application to real-world industrial scenarios is often limited by a number of factors. First, by the need of complex and expensive hardware. Second, by current limitations in the efficient collection, storage, annotation, and integration of the sensed data. Moreover, ML techniques, and especially deep learning, typically require to be trained on a large amount of annotated data (e.g., for image-based systems, a large amount of images of the powder bed per each possible defect and condition). Considering that the intentional production of defective parts is not viable in industry, as it is costly and time-consuming, the generation of a significant training set becomes an issue.

To address this problem, ML can be put at work even to create synthetic and realistic images, resembling the ones obtained during the print of a defective part [2]. In this regard, one of the most promising approaches is Generative Adversarial Network (GAN), a generative model characterized by training a pair of neural networks (a generator and a discriminator) in competition with each other [14]. Among the many families of GANs recently proposed by literature, Conditional GAN (CGAN) uses an additional input in the generator network to direct the generation process [27], obtaining very good results in many data augmentation tasks. While GANs are becoming very popular in many Computer Vision tasks, the application to the AM

sector is still limited. In [13], the authors developed a CGAN to produce synthetic data using as input the layer-by-layer images captured with a near-infrared high-resolution camera. As conditional images, the authors use a synthetic picture of the shape of the built artifact, and then they generate the corresponding near-infrared image, which mimics the characteristics of the captured ones. Ideally, a similar approach may be used for more complex tasks involving a large number of defects, like the one addressed by our case-study. More specifically, starting from an original image without flaws, CGAN can generate synthetic images of defects, augmenting the training set for defect classification. Unfortunately, the amount of data needed to train a standard CGAN for this purpose would not be much lesser than the one needed to train a classifier from scratch. To overcome this problem, in the present study a very promising architecture called ConSinGAN [19] is employed, that is able to learn generative models from a single training image (more details will follow in the next sections).

At present, the use of real-time monitoring systems in AM, coupled with Machine Learning models and, eventually, data augmentation strategies, is still mainly applied to the early detection of layer defects, for part qualification purposes. Given the lack of maturity of AM for mass production, little attention has been devoted so far to monitoring the status and health of the AM machine, for predictive maintenance purposes. Nonetheless, the extensive undergoing research in the field of sensing technology and ML models for AM defect analysis and process characterization is creating a solid background for future developments, where similar concepts may be easily applied to the early detection of machine anomalies and failure prediction. This is expected to enabled significant advantages in terms of reduced unnecessary post-processing analysis, equipment replacement, increased process safety, availability, and efficiency.

4 Case-study: layer-wise defects monitoring system for DMLS based on visible-range imaging

In this section, a fully-automated framework for layer-wise defects monitoring in DMLS AM is presented. The system is based upon an off-axis low-cost optical sensor for image acquisition of the powder bed and the manufactured object during the layering process. Then, a set of fully-automated tools based on Computer Vision and ML allow the detection of possible defects of the part that are hard to spot by visual inspection. The prototype was designed in a real-world industrial scenario and developed on top of a fully operative DMLS machine, in an automotive company. By allowing the early stopping/correction of the faulty artefacts, this system is expected to improve process repeatability and majorly reduce human intervention, with major positive impacts on the production costs.

Together with the data collection and the automated defects detection methods, a first prototype of synthetic image generation leveraging ConSinGAN is proposed,

which starts from the images acquired with the proposed fully-automated framework to produce synthetic images addressing two different types of powder bed defects.

4.1 Data acquisition and processing system

The implemented monitoring system is built upon low-cost hardware and camera on top of an EOS M290 DMLS printer in an automotive company. As shown in Fig. 4, it includes:

- an Arduino Uno computing platform directly connected with the 3D printer used to manage the system, trigger the camera, and take images of the powder bed.
- an IDS UI-1540-SE 1.31Mpix camera (1280 × 1024 resolution). The camera is triggered through the Application Programming Interface (API) made available by the manufacturer. The acquisition is off-axis with respect to the optical path of the laser.
- A standard PC running Linux, to collect images in the Portable Network Graphics (PNG) format with a resolution of 1280 × 1024 and run the image analytics algorithms.

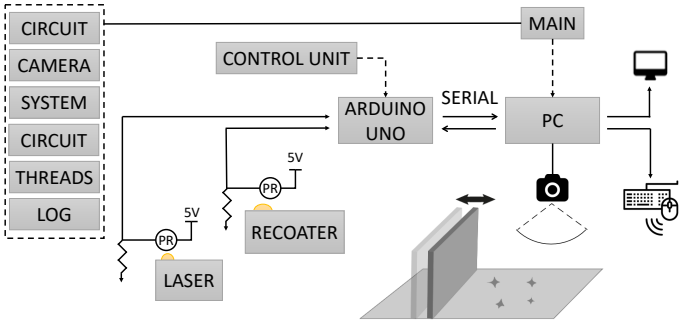

Fig. 4: In-situ monitoring system.

The image acquisition is automatically triggered by 3D printer states, exploiting the signals emitted respectively by the action of the laser and of the recoater, by means of photo-resistors. By doing so, the system is able to acquire images of the powder bed before and after each layer is printed, without requiring any user interaction.

4.2 Defects detection algorithms

The proposed solution includes a set of near real-time image analytic algorithms that allows the detection of five different powder bed defects, as well as continuous monitoring of the profile of the object that is being printed. The algorithms are based on image processing and Machine Learning and were developed in Python using OpenCV and Keras standard libraries.
Fig. 5 (a)-(e) show five main categories of defects targeted by our system:

- *Holes* (Fig. 5 (a)): localised lacks of metallic powder that create small dark areas in the powder bed image. The origin is a lack of powder due to bad regulation of the dosing factor.
- *Spattering* (Fig. 5 (b)): droplets of melted metal ejected from the melt pool and landed in the surroundings.
- *Incandescence* (Fig. 5 (c)): high-intensity areas in the completed layer image, resulting from an excess of laser energy density and a consequent inability by the melt pool to cool down correctly.
- *Horizontal* defects (Fig. 5 (d)): dark horizontal lines in the powder bed caused by the incorrect spreading of the powder, possibly because of the geometric imperfection of the piece or of the metallic powder.
- *Vertical* defects (Fig. 5 (e)): vertical undulation of the powder bed, consisting of alternated dark and light lines along the direction of the recoater's path. The origin is either a mechanical interference between the part and the recoater or a mechanical defect of the recoater's surface.

Each of these powder bed defects is known to cause either porosities or microstructural alterations in the printed parts, as well as lower mechanical characteristics.
The pipeline for run-time defects detection consists of several image processing steps.

- *Normalization* (Fig. 6 (a)): the images are first normalised against a common reference frame, in order to correct uneven illumination problems. To do so, an image of the powder bed is acquired before the start of the layering process and used as a reference throughout.
- *Contrast enhancement* (Fig. 6 (b)): a standard background subtraction algorithm is applied to make the objects more distinguishable from each other, as well as from the background [30].
- *Objects identification* (Fig. 6 (c)): intensity discontinuities are identified by means of automated intensity thresholding algorithm. This provides a rough identification of the different objects in an image.
- *Morphological filtering* (Fig. 6 (d)): specific objects are recognized based on their shape, exploiting morphological algorithms. More in detail, Watersheds, and Hough transform, followed by standard morphological regularization (i.e., opening, closing, holes filling), are respectively applied to identify round-shaped and horizontal/vertical lines. Based on the specific shape and number of detected objects, the software identifies a specific category of defect.

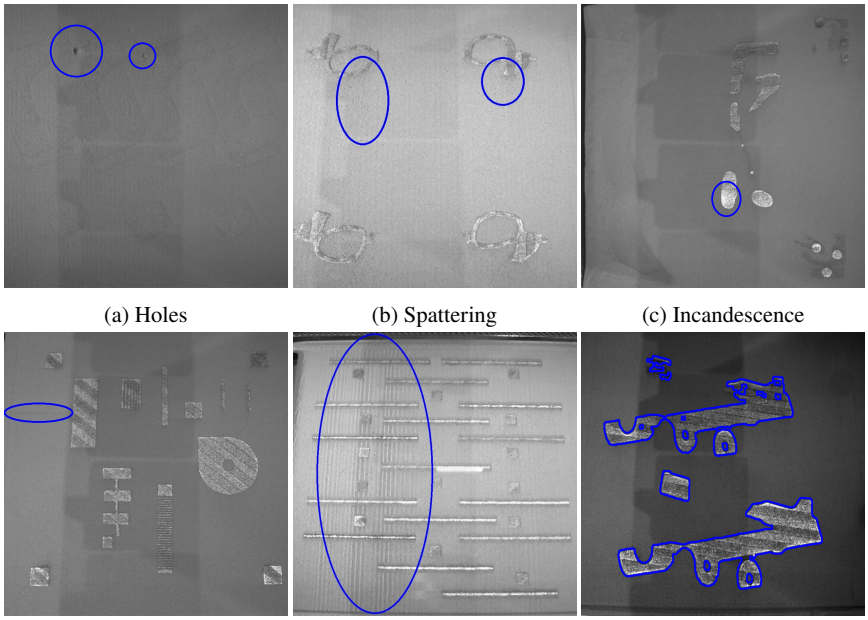

(a) Holes (b) Spattering (c) Incandescence

(d) Horizontal (e) Vertical (f) Profile monitoring

Fig. 5: (a)-(e) Examples of powder bed defects targeted by the system. (f) Profile monitoring example.

As an example, in Fig. 6 is presented the pipeline applied to detect a spattering defect, showing the outcome of each intermediate step. Spattering is indeed one of the defects that most frequently happen during powder bed fusion: it involves tiny particles of liquid metal being ejected from the laser's path, which may contaminate the powder bed and create issues such as porosity, roughness, and lack of adhesion in the finished parts. At the end of the last step in Fig. 6 (i.e. morphological filtering), the most relevant spatters are identified.

4.3 Part profile monitoring algorithm

Besides powder bed defects detection, the system includes a fully automated *profile monitoring* suite that is able to monitor the profile of the build on a layer-by-layer basis (see an example in Fig. 5 (f)). This task has additional algorithmic and computational challenges compared to basic powder bed defects because the printed parts may have very different shapes and dimensions.
In our solution, profile monitoring is addressed as a semantic segmentation problem. Semantic segmentation aims to cluster parts of an image together, which belong to the same object, using a pixel-level prediction to classify each pixel in an image

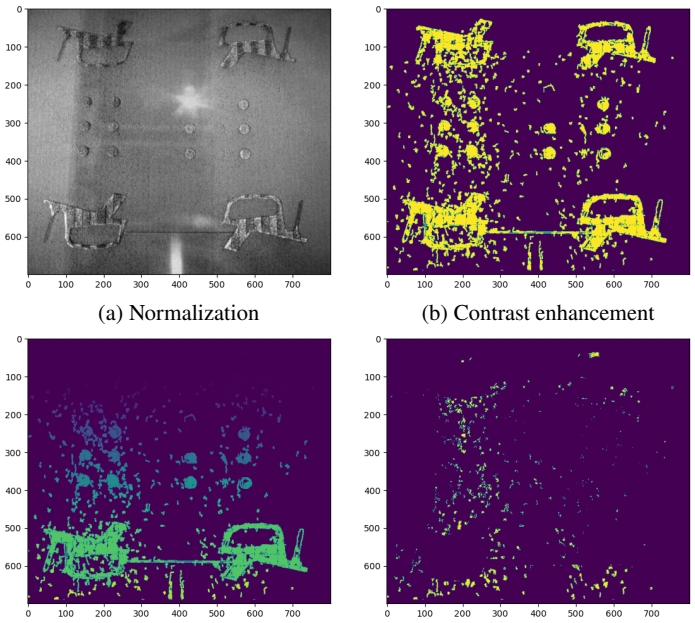

(a) Normalization (b) Contrast enhancement

(c) Objects identification (d) Morphological filtering

Fig. 6: Example of spattering defects detection pipeline.

according to a category. In other words, image segmentation becomes a binary classification task, where each pixel needs to be labeled as belonging to the object of interest (in our case, the printed part) or the powder bed.

To achieve this purpose, a U-Net architecture is employed [32], a deep learning algorithm that was initially designed for biomedical image segmentation and then successfully applied to many different Computer Vision applications. The network implements an end-to-end fully convolutional network (FCN) composed of convolutional and pooling layers without any dense layer, which makes it suitable for any image size. As shown in Fig. 7, the architecture is composed of two paths. The first path (encoding) is the contraction path or encoder used to capture the context in the image. It consists of a stack of various convolutional and max-pooling layers with gradually decreasing feature map dimension. The second path (decoding) is a symmetric expanding path or decoder used to enable precise localization using transposed convolutions. In the presented approach, the U-Net follows the implementation suggested by [32]. The encoding path consists of the repeated application of two 3×3 convolutions, with Rectified Linear Unit (ReLU) as activation function and a 2×2 max pooling operation. The decoding path consists of an upsampling of the feature map (up-conv) followed by a 2×2 convolution with ReLU as activation function, a concatenation with the correspondingly cropped feature map from the contraction path, and two 3×3 convolutions, each followed by a ReLU. The copy and crop are necessary due to the loss of border pixels in every convolution. At the final

layer, a 1×1 convolution is used to map each feature vector to the desired number of classes. In total, the network has 23 convolutional layers.

In this application, the two classes to be classified are the foreground (i.e., the printed part) and the background (i.e., the powder bed). First, it was used as input images with a size of 360×480. Then, the input size was fine-tuned on a validation set consisting of images of a representative PBF layer, and finally set the optimal size to 320×320.

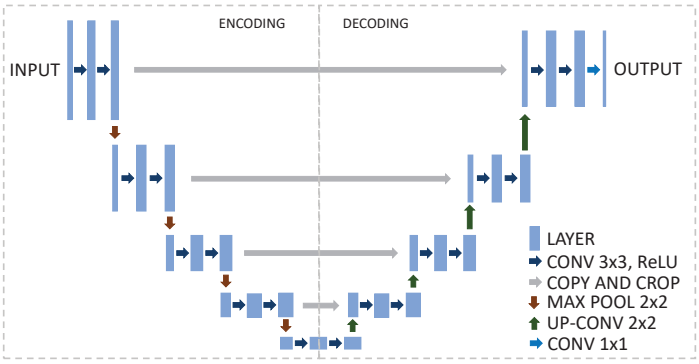

Fig. 7: U-Net architecture.

4.4 Dataset augmentation with GAN

Unfortunately, training ML algorithms to AM defect classification requires a large number of training images, with and without defects. As anticipated in Section 3, this is difficult to obtain in a real-world industrial setting, especially for the defect categories. To overcome this issue and increase the number of defective images available for the training, the discussed solution adopts an extended version of Conditional Generative Adversarial Network, ConSinGAN [19]. While traditional GANs still require large datasets for the training, ConSinGAN is able to generate synthetic data starting from a single image. This characteristic is of major importance, given the very limited number of defective images.

As shown in Fig. 8, a classic GAN architecture is composed of two Neural Networks, the Generator and the Discriminator, that compete to produce a generative model. The generator network produces synthetic data starting from the input, with the aim of obtaining data that resembles the real and available samples. At the same time, the discriminator network is a binary classifier that is trained to distinguish the synthetic samples produced by the generator from the real ones. The training phase consists of an adversarial process between the two networks, in which the generator tries to increase the error rate of the discriminator, while the latter tries to distinguish

real and synthetic data. Hence, the core idea is to implement an indirect training of the generative model through the discriminator: the generator has no direct access to real data, and interacts only with the discriminator [4].

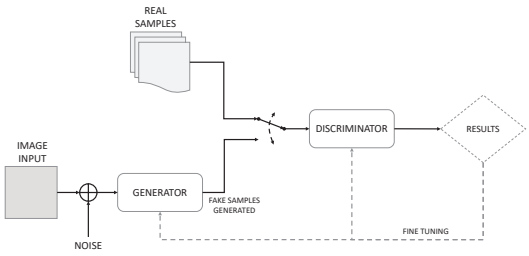

Fig. 8: Generative Adversarial Network architecture.

The ConSinGAN is structured in a multi-stage and multi-resolution approach, as shown in Fig. 9. First the ConSinGAN uses, as input for few iterations, an image with a coarse resolution to learn mapping a random noise vector z to a low-resolution image (See *Generator Phase 0* in Fig. 9). After the initial training has converged, the size of the generator is increased, adding three additional convolutional layers. Each stage takes as input the raw features from the previous stage, and a residual connection is used in each stage to feedforward the last convolutional layer (See *Stage 1* in Fig. 9). The process is repeated N times until the desired output resolution is reached. The synthetic image created by the generator is given as input to the discriminator, together with a real image from the dataset. The discriminator is trained to discern if the images given are real or synthetic, comparing them.

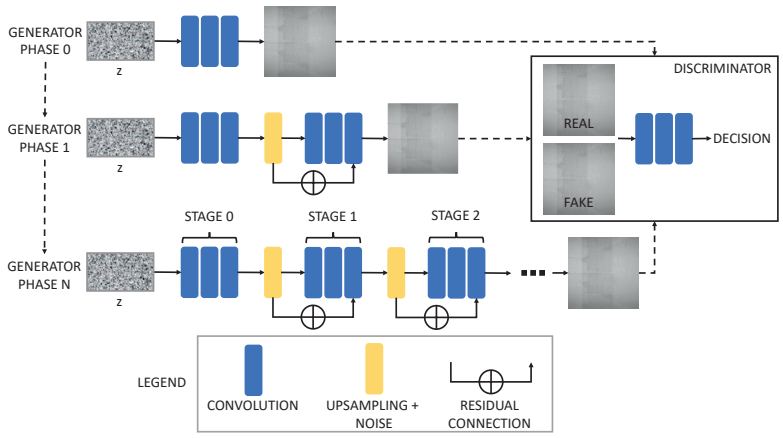

Fig. 9: ConSinGAN architecture [19].

The most critical part of the synthetic image generation is the image harmonization (see an example in Fig. 10). It consists in transforming a composite image, called naive (Fig. 10 (b)), into a realistic image by applying to the changes made the same style and appearance of the original image, called training (Fig. 10 (a)). The output of this process is a synthetic image similar to the original one (Fig. 10 (c)). To perform this process, the network is first trained to learn a generative model from the original image. Then, given the naive image as input, it tries to transform it into an image that should resemble the original learned distribution. Once the model is trained on a specific image, various synthetic images can be generated by varying only the naive picture.

(a) Training image (b) Naive image (c) Harmonized image

Fig. 10: Example of image harmonization [19].

Fig. 11 shows an example of AM image generation with the ConSinGAN. To generate new images presenting defects, the image harmonization process is carried out as follows: i) the generator is trained using a real image captured without defects (Fig. 11 (a)); ii) a naive image is created applying modifications to the training image by using a photo editing software (Fig. 11 (b)); iii) the naive images is harmonized to resemble the training image characteristics (Fig. 11 (c)). In this way, the synthetic defects are assimilated into the original image.

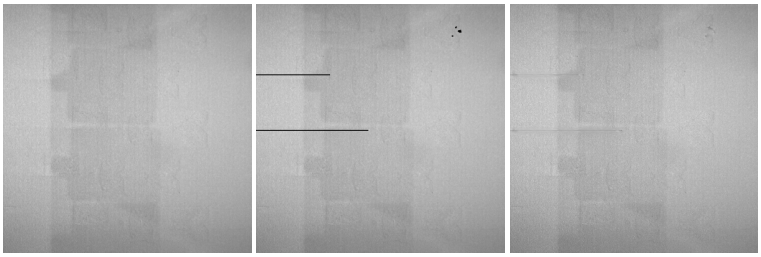

(a) Training image (b) Naive image (c) Synthetic image

Fig. 11: Example of image generation

The data generated can be used to increase the dataset available to both the train and validation phases of defect detection algorithms, breaking down the costs of generating a huge set of real defect data.

5 Experimental results

To validate the defect detection algorithms, a set of pre-annotated images was used with all the defects targeted by the proposed system. For the five main categories of defects, we run a statistical validation by analyzing whether the algorithm identified the defect or not, using metrics that are widely accepted in classification tasks:

- Accuracy: it represents the number of correct classifications with respect to the total cases.
$$Accuracy = \frac{TP + TN}{TP + TN + FP + FN}$$
- Precision: it is the fraction of relevant cases among the retrieved instances.
$$Precision = \frac{TP}{TP + FP}$$
- Recall: it is the fraction of the total amount of relevant instances that were retrieved.
$$Recall = \frac{TP}{TP + FN}$$

In this work, True Positives (TP) represent the instances when the algorithms were able to detect a defect that was really present. True Negatives (TN) represent the instances when a given defect was not present, and the algorithm was right in not detecting it. False Positive (FP) and False Negative (FN) represent the possible errors of the algorithms, respectively in detecting a defect that was not present, or not being able to identify a defect that was present. Table 1 reports the results obtained on a test set of 24 images with different powder bed conditions and defects.

Table 1: Defects detection algorithms validation

	Holes	**Spatt.**	**Incand.**	**Horizontal**	**Vertical**
TP	14	22	15	11	6
TN	8	1	4	11	16
FP	2	1	5	1	0
FN	0	0	0	1	2
Accuracy	91.3%	95.8%	79.2%	91.6%	91.67%
Precision	87.5%	95.6%	75%	91.6%	100%
Recall	100%	100%	100%	91.6%	75%

For all the five defects, the results of the metrics considered are $\geq$ 75% with the worst results for the Incandescence defects (Precision: 75%) and Vertical defects (Recall: 75%). According to our tests, Incandescence proved to be the most challenging defect to be recognized, probably due to the high pixel luminosity variation. On the other hand, Spattering defects are the easiest due to the high amount of spatters generated.

For the profile monitoring task, the validation exploits the Sørensen–Dice coefficient (DSC) to compare the profile segmentation obtained with our algorithm against a manually obtained ground truth. This metric is used to gauge a 0 to 1 similarity of two binary images, as follows:

$$DSC = \frac{2|X \cap Y|}{|X| + |Y|}$$

where $|X|$ and $|Y|$ are the number of pixels of the two images (in our case, the automatic segmentation and the ground truth) and $|X \cap Y|$ the number of pixels that are common to both images. Fig. 12 shows an example of this procedure, with (a) the binary mask obtained by manual segmentation, used as the ground truth, and (b) the binary mask obtained by our profile monitoring suite.

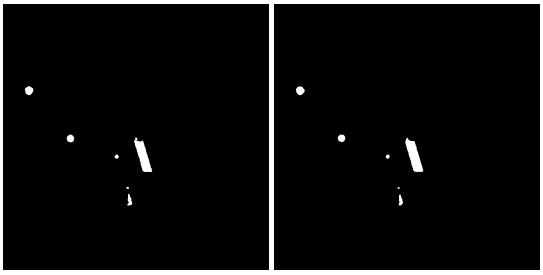

(a) Ground Truth (b) Automatic algorithm

Fig. 12: Profile monitoring: validation example.

In the conducted tests, a very good similarity between automated segmentation and manual ground truth was obtained, with mean DSC value equal to 0.878, when computed on each single segmented object, and to 0.911, when computed on each layer image taken as a whole.

Finally, Table 2 reports the execution time of all the tested algorithms. As can be seen from the reported values, execution times are all below 2.5s, which is well below the time elapsing between two subsequent layers. Profile monitoring is the algorithm taking the longest time (2.461s) because it involves running a deep neural network. The other algorithms, which exploit standard image processing operations, are all below 1s of execution.

As final step, the results of the synthetic data generation process were validated. In the implemented prototype, the image augmentation was preliminarily carried out

Table 2: Mean execution time of the algorithms.

Operation	Time [s]	Operation	Time [s]
Holes	0.791	**Horizontal**	0.593
Spattering	0.574	**Vertical**	0.932
Incandescence	0.821	**Profile monitoring**	2.461

on two types of defects: holes and horizontal. We assessed the results obtained by the ConSinGan through a most widely used GAN evaluation metric, that is the Fréchet Inception Distance (FID) [18]:

$$FID = ||\mu_X - \mu_Y||^2 + Tr(\Sigma_X + \Sigma_Y - 2\sqrt{\Sigma_X \Sigma_Y})$$

Where X is the set of real images, Y is the set of synthetic images; μ_X and μ_Y are the feature-wise mean of the real and generated images, respectively; Σ_X and Σ_Y are the covariance matrix for the real and generated feature vectors, respectively; Tr refers to the trace operation in matrix, which is the sum of the diagonal elements; $||\mu_X - \mu_Y||^2$ refers to sum squared difference between the two mean vectors.

The FID value ranges between 0 and plus infinite: a value near to 0 means that the two images are the same, while a very high value means that the two images are completely different.

Fig. 13 shows an example of a real image without defects (a) and a synthetic image (b) with holes defects, as generated by our approach. As it can be seen, the two images are quite similar, corresponding a FID value of 85.74.

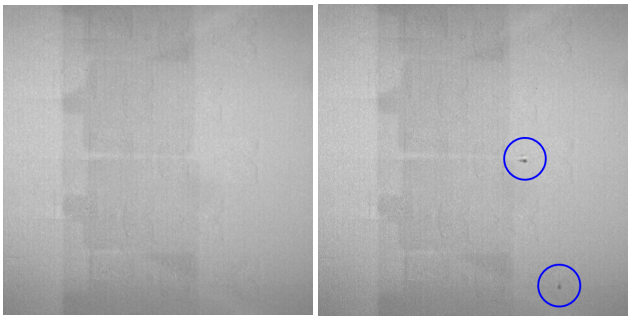

(a) Real image (b) Synthetic image

Fig. 13: Comparison between a training image and a synthetic one with defects (holes).

Table 3 reports the results obtained after 2000 steps, on a test set of 20 generated images with holes and horizontal defects. As expected, the FID shows similar results for all the generated images. This is due to the fact that the synthetic images were

generated starting from same training set, and that the added defects are quite similar. The FID values of the synthetic images are also quite small, demonstrating a good similarity to real ones with the same defects.

Table 3: ConSinGAN results

Synthetic image	1	2	3	4	5	6	7	8	9	10
FID	131.07	156.45	93.66	85.74	97.74	107.27	103.71	119.70	93.49	99.81
Synthetic image	11	12	13	14	15	16	17	18	19	20
FID	110.82	90.14	102.64	117.35	127.00	101.58	112.89	98.61	111.51	103.21

As a final experiment, the synthetic images were tested with the defects detection algorithms. Table 4 reports the results obtained on a test set of 24 synthetic images with holes and horizontal defects, generated with the ConSinGAN.

Table 4: Defects detection results on artificially generated images

	Holes	**Horizontal**
TP	8	8
TN	14	12
FP	1	2
FN	1	2
Accuracy	91.7%	83.3%
Precision	88.9%	80.0%
Recall	88.9%	80.0%

For both the defects, the results of the considered metrics (Accuracy, Precision, and Recall) are $\geq$ 80% with the worst results for the Horizontal defects (Precision and Recall: 80%). Hence, according to the experiments conducted, the defect detection results are similar to the results obtained with real images. The holes detection algorithm has better Accuracy and Precision with synthetic images (Accuracy: 91.6%, Precision: 88.9%) than with real images (Accuracy: 91.3%, Precision: 87.5%), while the Recall is better with the real images (Recall with synthetic images: 88.9%, Recall with real images: 100%). Instead, the horizontal detection algorithm has accuracy, precision and recall better with real images (Accuracy: 91.6%, Precision: 91.6%, Recall: 91.6%) than with synthetic images (Accuracy: 83.3%, Precision: 80.0%, Recall: 80.0%) Sure indeed, holes are easier to detect compared to horizontal defects, that can be easily confused with the powder bed background. However, on the test case with synthetic images, the metrics results for the horizontal defect were similar to those with real images, with a small reduction of performance $\leq$ 12% for the worst-case Recall.

6 Conclusion and future works

Computer Vision and ML have proven to be promising approaches for the in-situ monitoring of the AM process. Nonetheless, the actual use of these approaches in a real industrial scenario is still limited due to a number of challenges. First of all, the lack of effective data collection infrastructure specifically devoted to AM. Second, the necessity to train the models on large annotated datasets, which are typically costly and difficult to obtain in industrial environments.

This chapter presented a low-cost camera-based in-situ defects monitoring system for metal PBF and data generation. The preliminary prototype, developed and tested in a real industrial scenario of an automotive company, includes: i) a set of run-time Computer Vision and ML algorithms to detect five different categories of powder bed defects, as well as the layer-wise monitoring of the profile of a printed part and ii) a synthetic image generation model, for data augmentation purposes. Experimental results suggest that the algorithms have a good performance in terms of defect detection accuracy and profile segmentation and they are suitable for near real-time execution with low-cost hardware. The framework is currently being extended to provide layer-by-layer comparisons between the profile of the printed part (as returned by the profile monitoring suite) and the desired profile as defined by the slicer. This will allow a near real-time automated detection of any profile alterations during a build.

In its current form, the presented framework only allows the continuous monitoring of the AM part, and the timely detection of macroscopic defects based on the real-time comparison with a baseline. Nonetheless, the continuous growth of collected images is creating a solid ground for future extensions in the direction of predictive analytics. In this regard, it is planned to integrate the available image dataset with process parameters as well as with post-process information (i.e., results of quality and mechanical tests on the finished parts, as well as historical information about part breakdowns), in order to train models able to predict and possibly correct the failure of a part, applying process optimization strategies.

References

1. Mukesh Agarwala, David Bourell, Joseph Beaman, Harris Marcus, and Joel Barlow. Direct selective laser sintering of metals. *Rapid Prototyping Journal*, 1995.
2. Kosmas Alexopoulos, Nikolaos Nikolakis, and George Chryssolouris. Digital twin-driven supervised machine learning for the development of artificial intelligence applications in manufacturing. *International Journal of Computer Integrated Manufacturing*, 33(5):429–439, 2020.
3. Masoumeh Aminzadeh and Thomas R Kurfess. Online quality inspection using bayesian classification in powder-bed additive manufacturing from high-resolution visual camera images. *Journal of Intelligent Manufacturing*, 30(6):2505–2523, 2019.
4. Martin Arjovsky and Léon Bottou. Towards principled methods for training generative adversarial networks. *arXiv preprint arXiv:1701.04862*, 2017.

5. Mohsen Attaran. The rise of 3-d printing: The advantages of additive manufacturing over traditional manufacturing. *Business Horizons*, 60(5):677–688, 2017.
6. Ivanna Baturynska, Oleksandr Semeniuta, and Kristian Martinsen. Optimization of process parameters for powder bed fusion additive manufacturing by combination of machine learning and finite element method: A conceptual framework. *Procedia CIRP*, 67:227–232, 2018.
7. I Campbell, Olaf Diegel, J Kowen, and T Wohlers. *Wohlers report 2018: 3D printing and additive manufacturing state of the industry: annual worldwide progress report*. Wohlers Associates, 2018.
8. Volker Carl. Monitoring system for the quality assessment in additive manufacturing. In *AIP Conference Proceedings*, volume 1650, pages 171–176. American Institute of Physics, 2015.
9. Chee Kai Chua, Kah Fai Leong, and Chu Sing Lim. *Rapid prototyping: principles and applications (with companion CD-ROM)*. World Scientific Publishing Company, 2010.
10. European Commission. Additive manufacturing in fp7 and horizon 2020, 2014.
11. Luiz Jonatã Pires de Araújo, E. Özcan, Jason A. D. Atkin, M. Baumers, C. Tuck, and R. Hague. Toward better build volume packing in additive manufacturing: classification of existing problems and benchmarks. In *Annual International Solid Freeform Fabrication Symposium*. Austin, Texas, USA, 2015.
12. Mia Delic and Daniel R Eyers. The effect of additive manufacturing adoption on supply chain flexibility and performance: An empirical analysis from the automotive industry. *International Journal of Production Economics*, 228:107689, 2020.
13. Christian Gobert, Edel Arrieta, Adrian Belmontes, B. Ryan Wicker, Francisco Medina, and Brandon McWilliams. Conditional generative adversarial networks for in-situ layerwise additive manufacturing data. In *Proceeding of the 29th international Solid Freeform Fabrication Symposium*, 2019.
14. Ian Goodfellow, Jean Pouget-Abadie, Mehdi Mirza, Bing Xu, David Warde-Farley, Sherjil Ozair, Aaron Courville, and Yoshua Bengio. Generative adversarial nets. In *Advances in neural information processing systems*, pages 2672–2680, 2014.
15. Marco Grasso, Francesco Gallina, and Bianca Maria Colosimo. Data fusion methods for statistical process monitoring and quality characterization in metal additive manufacturing. *Procedia CIRP*, 75:103–107, 2018.
16. Nannan Guo and Ming C Leu. Additive manufacturing: technology, applications and research needs. *Frontiers of Mechanical Engineering*, 8(3):215–243, 2013.
17. FN Habib, P Iovenitti, SH Masood, and M Nikzad. Fabrication of polymeric lattice structures for optimum energy absorption using multi jet fusion technology. *Materials & Design*, 155:86–98, 2018.
18. Martin Heusel, Hubert Ramsauer, Thomas Unterthiner, Bernhard Nessler, and Sepp Hochreiter. Gans trained by a two time-scale update rule converge to a local nash equilibrium. *Advances in neural information processing systems*, 30:6626–6637, 2017.
19. Tobias Hinz, Matthew Fisher, Oliver Wang, and Stefan Wermter. Improved techniques for training single-image gans. *arXiv preprint arXiv:2003.11512*, 2020.
20. Ahmed Hussein, Liang Hao, Chunze Yan, Richard Everson, and Philippe Young. Advanced lattice support structures for metal additive manufacturing. *Journal of Materials Processing Technology*, 213(7):1019–1026, 2013.
21. Paul Francis Jacobs. *Rapid prototyping & manufacturing: fundamentals of stereolithography*. Society of Manufacturing Engineers, 1992.
22. MW Khaing, JYH Fuh, and L Lu. Direct metal laser sintering for rapid tooling: processing and characterisation of eos parts. *Journal of Materials Processing Technology*, 113(1-3):269–272, 2001.
23. L Jyothish Kumar and CG Krishnadas Nair. Current trends of additive manufacturing in the aerospace industry. In *Advances in 3D printing & additive manufacturing technologies*, pages 39–54. Springer, 2017.
24. Zhixiong Li, Ziyang Zhang, Junchuan Shi, and Dazhong Wu. Prediction of surface roughness in extrusion-based additive manufacturing with machine learning. *Robotics and Computer-Integrated Manufacturing*, 57:488–495, 2019.

25. Hod Lipson and Melba Kurman. *Fabricated: The new world of 3D printing*. John Wiley & Sons, 2013.
26. Mahesh Mani, Brandon M Lane, M Alkan Donmez, Shaw C Feng, and Shawn P Moylan. A review on measurement science needs for real-time control of additive manufacturing metal powder bed fusion processes. *International Journal of Production Research*, 55(5):1400–1418, 2017.
27. Mehdi Mirza and Simon Osindero. Conditional generative adversarial nets. *arXiv preprint arXiv:1411.1784*, 2014.
28. Bernhard Mueller and Detlef Kochan. Laminated object manufacturing for rapid tooling and patternmaking in foundry industry. *Computers in Industry*, 39(1):47 – 53, 1999.
29. Lawrence E. Murr, Sara M. Gaytan, Diana A. Ramirez, Edwin Martinez, Jennifer Hernandez, Krista N. Amato, Patrick W. Shindo, Francisco R. Medina, and Ryan B. Wicker. Metal fabrication by additive manufacturing using laser and electron beam melting technologies. *Journal of Materials Science & Technology*, 28(1):1 – 14, 2012.
30. Wan Azani Mustafa and Haniza Yazid. Image enhancement technique on contrast variation: a comprehensive review. *Journal of Telecommunication, Electronic and Computer Engineering (JTEC)*, 9(3):199–204, 2017.
31. Tanisha Pereira, John V Kennedy, and Johan Potgieter. A comparison of traditional manufacturing vs additive manufacturing, the best method for the job. *Procedia Manufacturing*, 30:11–18, 2019.
32. Olaf Ronneberger, Philipp Fischer, and Thomas Brox. U-net: Convolutional networks for biomedical image segmentation. In *International Conference on Medical image computing and computer-assisted intervention*, pages 234–241. Springer, 2015.
33. Mika Salmi, Kaija-Stiina Paloheimo, Jukka Tuomi, Jan Wolff, and Antti Mäkitie. Accuracy of medical models made by additive manufacturing (rapid manufacturing). *Journal of Cranio-Maxillofacial Surgery*, 41(7):603–609, 2013.
34. Luke Scime and Jack Beuth. A multi-scale convolutional neural network for autonomous anomaly detection and classification in a laser powder bed fusion additive manufacturing process. *Additive Manufacturing*, 24:273–286, 2018.
35. Sergey A Shevchik, Christoph Kenel, Christian Leinenbach, and Kilian Wasmer. Acoustic emission for in situ quality monitoring in additive manufacturing using spectral convolutional neural networks. *Additive Manufacturing*, 21:598–604, 2018.
36. Jorge VL Silva and Rodrigo A Rezende. Additive manufacturing and its future impact in logistics. *IFAC Proceedings Volumes*, 46(24):277–282, 2013.
37. Douglas S Thomas and Stanley W Gilbert. Costs and cost effectiveness of additive manufacturing. *NIST special publication*, 1176:12, 2014.
38. Xin Wang, Man Jiang, Zuowan Zhou, Jihua Gou, and David Hui. 3d printing of polymer matrix composites: A review and prospective. *Composites Part B: Engineering*, 110:442 – 458, 2017.
39. Dongsen Ye, Geok Soon Hong, Yingjie Zhang, Kunpeng Zhu, and Jerry Ying Hsi Fuh. Defect detection in selective laser melting technology by acoustic signals with deep belief networks. *The International Journal of Advanced Manufacturing Technology*, 96(5-8):2791–2801, 2018.
40. Seung-Schik Yoo. 3d-printed biological organs: medical potential and patenting opportunity, 2015.
41. Yingjie Zhang, Geok Soon Hong, Dongsen Ye, Kunpeng Zhu, and Jerry YH Fuh. Extraction and evaluation of melt pool, plume and spatter information for powder-bed fusion am process monitoring. *Materials & Design*, 156:458–469, 2018.
42. Zuowei Zhu, Nabil Anwer, Qiang Huang, and Luc Mathieu. Machine learning in tolerancing for additive manufacturing. *CIRP Annals*, 67(1):157–160, 2018.